Mapping the functional connectome traits of levels of consciousness.

Enrico Amico[a,b], Daniele Marinazzo[b], Carol DiPerri[a,c], Lizette Heine[a,c], Jitka Annen[a,c], Charlotte Martial[a,c], Mario Dzemidzic[d], Steven Laureys[a,c,*] and Joaquín Goñi[e,f,g,*]

[a]Coma Science Group, GIGA Research Center, University of Liège, Liège, Belgium

[b]Department of Data-analysis, University of Ghent, B9000 Ghent, Belgium

[c]University Hospital of Liège, Liège, Belgium

[d]Department of Neurology and Radiology and Imaging Sciences, Indiana University School of Medicine, Indianapolis, IN, USA

[e]School of Industrial Engineering, Purdue University, West-Lafayette, IN, USA

[f]Weldon School of Biomedical Engineering, Purdue University, West-Lafayette, IN, USA

[g]Purdue Institute for Integrative Neuroscience, Purdue University, West-Lafayette, IN, USA

*Authors contributed equally.

steven.laureys@ulg.ac.be

jgonicor@purdue.edu

Classification: NEUROSCIENCE

Keywords: fMRI, Brain Connectivity, Network Science, Consciousness

Short title: Mapping the functional traits of consciousness.

This is the author's manuscript of the article published in final edited form as:

Amico, E., Marinazzo, D., Di Perri, C., Heine, L., Annen, J., Martial, C., … Goñi, J. (2017). Mapping the functional connectome traits of levels of consciousness. NeuroImage, 148, 201–211. https://doi.org/10.1016/j.neuroimage.2017.01.020

Abstract

Examining task-free functional connectivity (FC) in the human brain offers insights on how spontaneous integration and segregation of information relate to human cognition, and how this organization may be altered in different conditions, and neurological disorders. This is particularly relevant for patients in disorders of consciousness (DOC) following severe acquired brain damage and coma, one of the most devastating conditions in modern medical care.

We present a novel data-driven methodology, *connICA*, which implements Independent Component Analysis (ICA) for the extraction of robust independent FC patterns (FC-traits) from a set of individual functional connectomes, without imposing any a priori data stratification into groups.

We here apply *connICA* to investigate associations between network-traits derived from task-free FC and cognitive/clinical features that define levels of consciousness. Three main independent FC-traits were identified and linked to consciousness-related clinical features. The first one represents the functional configuration of an “awake resting” brain, and is associated to the level of arousal. The second FC-trait reflects the disconnection of the visual and sensory-motor connectivity patterns and relates to the ability of communicating with the external environment. The third FC-trait isolates the connectivity pattern encompassing the fronto-parietal and the default-mode network areas as well as the interaction between left and right hemisphere, which are also associated to the awareness of the self and its surroundings.

Each FC-trait represents a distinct functional process with a role in the degradation of conscious states in functional brain networks, shedding further light on the functional sub-circuits that get disrupted in severe brain-damage.

Significance Statement

In this study we propose a novel methodology for the analysis of functional brain connectomes, namely connICA, which consists of the extraction of robust independent patterns of functional connectivity between cortical areas in healthy and diseased human brains. We apply connICA to investigate associations between robust functional traits and

cognitive/clinical features that define levels of consciousness based on resting-state fMRI connectivity in patients at different levels of consciousness after severe brain damage.

The versatility and simplicity of the connICA framework presented here constitute a powerful approach to extract and disentangle underlying functional processes embedded within healthy and diseased human brains, which might pave the way for innovative and clinically highly relevant brain connectivity analyses.

\body

Introduction

Disorders of consciousness (DOC) remain among the most challenging and poorly understood conditions in modern medical care. The term spreads over several pathological states qualified by dissociation between awareness and arousal (1, 2). Among these, patients in coma show no signs of awareness nor arousal; patients with unresponsive wakefulness syndrome/vegetative state (UWS) show no signs of awareness but do have an altered sleep and wake cycle; patients in a minimally conscious state (MCS) retain minimal non-reflexive and highly fluctuating signs of awareness. When patients regain functional object use and/or reliable communication they are referred to as emerging from MCS (EMCS) (3, 4). A particular outcome is represented by patients with a locked-in syndrome (LIS), who have no means of producing speech, limb or facial movements (except mostly for eye movement and/or blinking) but are still awake and fully conscious (5, 6). To date, the most validated diagnosis of these patients is based on the behavioral presentation of the patient. The distinction between these pathological levels of consciousness can be very challenging, as the boundaries between these states are often uncertain and ambiguous (4).

In the last decade, advances in neuroimaging techniques have allowed the medical community to gain important insights into the pathophysiology of DOC and to observe that altered states of consciousness are related to complex disruptions in the functional and structural organization of the brain (7-11).

At the same time, quantitative analysis based on complex networks have become more commonly used to study the brain as a network (12), giving rise to the area of research so

called Brain Connectomics (13, 14). In brain network models, nodes correspond to grey-matter regions (based on functional or structural, atlas-based parcellations that constitute a partition).while links or edges correspond either to structural connections as modeled based on white matter fiber-tracts or to the functional coupling between brain regions while subjects are either at rest or performing a task (15). Recent advances in functional neuroimaging have provided new tools to measure and examine *in vivo* the whole-brain temporal dependence of the dynamics of anatomically separated brain regions, defined as functional connectivity (FC) (16-18).

In parallel to the development of methods and network features in Brain Connectomics, analyses of functional magnetic resonance imaging (fMRI) data based on independent component analysis (ICA) have become an increasingly popular voxel-level approach (19). ICA, by relying upon a general assumption of independence, is a powerful and versatile data-driven approach for studying the brain, at temporal and spatial scales (20).

Examining functional connectivity in the human brain can give insight on how integration and segregation of information relates to human behavior and how this organization may be altered in diseases (7, 21). In the case of disorders of consciousness, voxel-level ICA-based fMRI studies of levels of consciousness in DOC patients have mainly shown alterations in the functional connectivity of the default mode network area (DMN) (22-24). Recent studies have also shown disrupted functional connectivity in resting state networks other than DMN (25) and possibility to correctly classify patients based on the level of connectivity of the “auditory” network (26).Furthermore, analyses of the functional networks of comatose brains have also evidenced a radical reorganization of high degree “hub” regions (27) and that most of the affected regions in patients belonged to highly interconnected central nodes (11, 28).

The potential of functional connectivity (FC) in particular and Brain Connectomics in general in exploring the diseased human brain as a network going through systemic changes is undisputed. However, there is still no clear way to accomplish two critical steps. of great clinical importance. First, separate underlying FC patterns representing different functional mechanisms and, second, relate those FC patterns or subsequent network features to individual cognitive performance or clinical evaluations. This is specially the case when studying a continuum of states, where the stratification of the cohort-subjects into categories

or groups is inappropriate and/or poorly defined. Furthermore, standard FC techniques are not able to model and disentangle common underlying forces or competing processes arising from different functional patterns of healthy and diseased human brains in a data-driven fashion, as for instance ICA does in the case of fMRI voxel time series (19, 20). This was indeed our motivation for the approach presented here.

In this study we bridge this gap by presenting a novel data-driven methodology, *connICA*, which consists of the extraction of robust independent patterns (traits) from a set of individual functional connectomes (see scheme in Figure 1). In this sense, *connICA* is a multiplex network framework both in the input (i.e., layers are individual FC connectomes) and in the output (i.e., layers are independent patterns or FC-traits). Here we apply *connICA* to investigate the link between cognitive/clinical features that define states of consciousness and resting-state functional connectivity (FC) data. The method allows the assessment of individual FC patterns (or FC layers) in a joint data-driven fashion providing as outputs multivariate independent FC-traits, which model independent sources or phenomena present in the input (i.e. the aforementioned individual FC patterns). In a final step, we assess the predictability of the weights (fingerprints) of each FC-trait on each subject from demographic and consciousness related variables, allowing for a continuous mapping of levels of consciousness within functional connectomes.

Results

Following individual subject BOLD fMRI data processing (see Figure S1 for examples of four individual sessions) and subsequent modeling of the individual task-free functional connectomes, connICA (see scheme at Figure 1) was run on the cohort of 88 subjects (32 conscious controls and 56 severely brain-damaged patients at different levels of consciousness; see Methods for details) without imposing any *a priori* information or stratification into groups. The procedure included 100 runs of *connICA* and allowed us to identify a total of 5 robust FC-traits (see Figure S2). In other words, they were present with high frequency and reproducibility across runs (see connICA section in Methods for details). Each FC-trait consists of two elements: an FC map of the same dimensions as an individual FC matrix with connectivity units being unitless and represented by weights, and a vector indicating the *amount* of the FC-trait present on each individual functional connectome (i.e.

the weight of the trait on each subject). Importantly, this latter *connICA* outcome allows us to associate individual cognitive and clinical features to each trait. Each of these 5 components (FC-traits) was then evaluated in terms of explained FC variance and Newman's modularity quality function Q (29) generalized for signed networks (30) with respect to the partition into RSNs proposed by Yeo and colleagues (31). The highest explained variance components were 1, 2 and 4, with a dominant FC-trait 1 explaining 18% of variance on average. It is important to note that the FC explained variance does not quantify the meaningfulness of the FC-trait with respect to the variables of interest (i.e. those related to levels of consciousness in this case), but only the average prominence of the trait in the set of the FC connectivity matrices extracted from the population of subjects.

Of the 5 extracted traits, both FC-traits 1 and 2 had a high modularity ratio Q score (see Figure 2A), which denotes that both FC traits have a strong fingerprint on the underlying RSNs organization (see insert in Figure 2B) in functional communities. We focused our subsequent analysis on FC traits 1, 2 and 4, which were the ones with highest R^2 and at the same time captured different aspects of the RSNs modular architecture.

The dominant FC-trait extracted using *connICA* (i.e. the one with the highest explained FC variance in the cohort) is shown in Figure 3D. Interestingly, it conforms to all the connectivity blocks or modules of the resting-state functional networks (RSNs, see insert Figure 2B) as introduced by Yeo and colleagues (31). For this reason, this FC-trait was denominated the *RSNs* trait. An incremental multi-linear model predicting the weight or *quantity* of the *RSNs* trait on each subject (see Figure 3A) was used, based on up to 7 predictors (see Figure 3G). A significant association with arousal, a subscore of the Coma Recovery Scale-Revised (CRS-R) (32-34), was found, after controlling for age, gender, traumatic brain injury (TBI), sedation, onset and CRS-R total score (with none of them being significant terms). In other words, the more aroused the subject (Figure 3G), the higher the subject-weight associated to the *RSNs* trait and hence the higher the presence of such trait. This might be due to the fact that this trait is reflecting a functional configuration of an *awake resting* brain. Therefore, this configuration might give a significant fingerprint for discriminating the “baseline wakefulness activity” of a human brain.

The other two FC-traits linked to cognitive features associated with levels of consciousness (i.e. the CRS-R total score and the communication subscore (32, 33)) are shown in Figure 3E and 3F.

In particular, the FC-trait depicted in Figure 3E mainly captures changes of intra-hemispheric functional connectivity in the visual and sensory motor networks across subjects in different levels of consciousness. We will refer to it as the *VIS-SM* trait. A significant link with the CRS-R communication subscore (32, 33) was found, as well as with three other variables previously added to the multilinear model (precisely with TBI, sedation and onset, see Figure 3H).

The positive sign of the beta coefficient associated to the communication subscore indicates that the trend of the linear fit follows the correspondent individual weights of the FC trait. In other words, the higher the communication subscore of a subject, the higher the contribution or presence of the *VIS-SM* trait in his/her functional connectome (Figure 3B). Interestingly, when adding etiology, sedation and time since onset (quantified here as the inverse of the days since the insult, see Methods), the explained variance of the model significantly increased. The negative sign of the associated beta coefficients for the three nuisance variables indicates a negative slope in the fit with the FC individual weights. That is, in the case of etiology, TBI patients have a lower amount of the *VIS-SM* trait in their functional connectomes; in the case of sedation, sedated patients have a lower contribution of the trait on their individual FC patterns; in the case of time since onset, the more recent the insult, the lower the prominence of the *VIS-SM* trait on the individual FC of the patient.

The trait shown in Figure 3F mainly captures modifications in the connectivity between DMN and fronto-parietal networks (hence denominated *FP-DMN* trait). Interestingly, the *FP-DMN* trait is linked to the CRS-R sum of scores, but also to the CRS-R communication subscore, even when the sum of scores is already added to the multilinear model (Figure 3I). The positive sign of the beta coefficient associated to these two predictors indicates that the higher the CRS-R sum of scores (communication subscore) for a subject, the higher the presence of the *FP-DMN* trait on his functional connectome. Notably, as one goes lower in the levels of consciousness, the contribution of the *FP-DMN* trait on the FC of a subject flips sign from negative to positive_–(see the sorted individual weights associated to *FP-DMN* trait,

Figure 3C, 3F). There is an analogous effect in a few subjects for the *VIS-SM* trait (Figure 3B, 3E).

The *RSNs* trait was mostly characterized by the underlying RSNs. We further characterized *VIS-SM* and *FP-DMN* traits by identifying the regions with a higher functional strength. The strength of participation of each brain region to the two FC-traits was measured as its absolute weighted degree (i.e. computed as the sum over columns of the absolute value of the FC-trait). The higher the strength, the more influential is the role of the brain region to the FC-trait, and hence to the disruption of the level of consciousness. *VIS-SM* trait mainly involves the occipital and visual areas, whereas fronto-parietal areas are the most involved in the *FP-DMN* trait (Figure 4).

Further analyses were performed on *VIS-SM* and *FP-DMN* traits to assess the presence of communities (Figure 5) by using consensus clustering (35) over 100 modularity solutions computed using the Louvain algorithm (36) with quality function Q extended to signed networks (30) (see Methods). Note that the obtained modular configuration gives insights on the data-driven organization of the functional cores common to the whole cohort. When going back to the individual space, the multiplication by the subject's weight may preserve or change this core modular organization depending on the sign (i.e. it changes the FC-trait signed network, see Figure 3). Hence, performing consensus clustering on the FC-traits allowed us to track the "normal conscious" (positive weights) configuration that gets disrupted towards "lower altered" (negative weights) levels of consciousness (Fig. 3A, 3B, 3C).

We looked at the prominence of each community by averaging the correspondent connectivity values within each module. Interactions between every two communities in the FC-traits were then evaluated by averaging the connectivity values connecting them, hence providing a representation of the "coupling" between communities.

For both traits, the highest modularity was associated to partitions of three modules. In line with results of Figure 4, the most influential module (the highest within-module average) for the *VIS-SM* trait appears to be the one comprising the occipital cortex and higher order visual areas. Notably, the latter is strongly decoupled from the DMN module (highest between-modules negative connectivity, Figure 5B), suggesting that in a healthy brain these two

modules are negatively correlated. This modular configuration is then altered after modifications of levels of consciousness.

The modular organization of *FP-DMN* trait revealed a substantial division of the brain in two hemispheres. The between-modules average weight shows that the most “antagonistic” communities encompass the two different hemispheres (Figure 5D), indicating that in normal consciousness the hemispheres are also anti-correlated. This “decoupling” or negative inter-module connectivity might change (i.e. it turns to positive, Figure 3C, 3F) following loss of consciousness.

Discussion

In this work we applied a novel data-based methodology, *connICA*, to the field of Brain Connectomics. Our approach is based on extracting independent connectivity traits from a set of individual functional connectomes to extract and map robust independent mechanisms or processes that explain the FC patterns of an entire cohort of subjects, without setting any *a priori* stratification into groups. We used the *connICA* framework to assess rsfMRI in 88 subjects with different levels of consciousness: 32 conscious controls and 56 severely damaged patients (2 coma, 17 UWS, 20 MCS, 13 EMCS, 4 LIS) of different etiology and duration, 31 of whom were acquired while receiving sedative drugs to control for movement artifacts. We investigated the functional connectivity traits underlining specific sensorimotor/cognitive capacities related to consciousness.

We showed how these traits separate the FC data into network subsystems with significant associations to levels of consciousness. Notably, this methodology allowed us to map and match the most meaningful functional traits to consciousness-related predictors taken at the patient’s bedside. This approach established the link between the alteration of levels of consciousness and the connectivity core associated to it.

The *connICA* framework provides a multiplex data-driven way to extract and compact (dimensionality reduction) the most meaningful multivariate information contained in the functional connectomes in a relatively small set of connectivity traits. In this work we showed how the modification of levels of consciousness is associated to specific connectivity disruptions using as reference seven widely accepted RSNs (i.e., visual, somatomotor, dorsal attention, ventral attention, limbic system, fronto-parietal, default mode network (31), and for

completeness, also subcortical regions (SUBC) and cerebellum (CER), see insert in Figure 2B).

One additional advantage of this approach is that the dimensionality of the output is significantly reduced, both in the number of the robust components extracted with respect to the initial population size (in the study analyzed here, 5 FC-traits starting from 88 FC matrices) and in the number of variables to be encoded in the multi-linear models, hence notably decreasing number of multiple comparisons. As opposed to univariate approaches mapping up to *N(N-1)/2* functional connections and their subsequent multi-linear models (*N* being the number of brain regions), the multi-layered output of *connICA* allows to focus on a small subset of robust FC-traits (by definition, a subset smaller or equal to the number of components set). This dimensionality reduction does not compromise but rather considerably facilitates the interpretability of the results, by compressing the individual variability into the most meaningful independent functional cores. It is noteworthy that most if not all the traits would have been missed with a standard group-average analysis of the functional connectomes.

By using connICA, we extracted three independent functional connectivity traits linked to cognitive features of levels of consciousness. Below is a characterization of each FC-trait and its association to different aspects of consciousness.

The *RSNs* trait (Figure 3D) is also the one which explains the most of the FC variance (Figure 2A) and is the closest to the Yeo's RSNs organization (31). It seems mainly associated to a global drop in the functional connectivity within each of the networks, and correlates with the CRS-R arousal subscore. We might think of this trait as the one of an *awake resting brain*. It reflects the connectivity organization of a functioning brain, which might be at least partially driven by its underlying structural connectivity (37-39).

The *VIS-SM* trait seems more associated to the effect of the pathology (i.e. etiology, time since onset) and the sedation level (Figure 3H). It shows a more prominent disruption in the occipital and sensorimotor areas as the level of consciousness decreases (Figure 3E), and it also correlates with functional communication (Figure 3H). Interestingly, the modularity analysis suggests that visual areas and DMN are anti-correlated in normal wakefulness (Figure 4A, 4B), stressing the importance of the interaction between the so called sensory

“slave” regions (40) and higher order cognitive regions as the DMN, for consciousness and functional communication (11). This corroborates the hypothesis that loss of consciousness might correlate with the disruption of primary sensory areas and higher-order associative cortices, which are thought to be required for conscious perception (i.e. global workspace, (26, 41)).

However, the recovery of this connectivity pattern seems not a sufficient condition for the restoration of levels of consciousness. Another independent functional trait appears to be linked to behavioral assessment of levels of consciousness, particularly to both the CRS-R total score and the communication subscore (*FP-DMN* trait, Figure 3F).

The *FP-DMN* trait captures changes in the anti-correlation between the FP-DMN networks. Notably, as one goes towards the deepest unconsciousness, the FP-DMN anti-correlation decreases, until the point where it “flips” to positive correlation, (see Figure 3C, 3F). This is in line with previous studies showing decreasing anti-correlation in anesthesia (42, 43), sleep (44) and UWS patients (45). Particularly, a recent study (46) showed that negative connectivity between DMN and FP networks was significantly different between patients and healthy controls. Indeed, UWS and MCS patients showed a pathological positive connectivity between these two networks, whereas patients who emerged from MCS and recovered a level of consciousness sufficient for functional communication and/or object use, exhibited partial preserved between-network negative connectivity (46). In this respect, the fact that the *FP-DMN* trait is strongly correlated to the communication subscore corroborates the idea that recovery of the FP-DMN between-network negative connectivity is prerequisite in order to regain functional communication.

Notably, the modularity analysis on *FP-DMN* trait reveals that the *decoupling* between the two hemispheres (Figure 5C) represents a “healthy” way of communication between left and right brain areas. The anti-correlation between hemispheres tends to disappear (i.e. goes towards zero or even positive correlation, see the individual weights of *FP-DMN* trait in Figure 3C) as levels of consciousness decrease.

Indeed, there is evidence suggesting that communication and coordination between the two hemispheres is essential for consciousness and conscious perception (47). It has been reported that transection of corpus callosum in refractory epileptic patients (i.e. split brain

patients) caused each hemisphere to have its own separate perception, concepts, and impulses to act (48). The conscious abilities of the two hemispheres are strongly differentiated in specialized cognitive modules (49), modulated by the thalamo-cortical system (subcortical regions are also split in left and right modules in *FP-DMN* trait, see Figure 5C). In this study we show that the interaction between specialized modules, as the VIS-SM interaction with DMN or the FP-DMN between-networks negative connectivity, is crucial for the emergence of consciousness. Perhaps this laterality enhances the complexity of ongoing brain processes and facilitates demanding cognitive processes such as consciousness of the self and the surrounding.

Taken together, these findings suggest that the connectivity core which differentiates across levels of consciousness is a combination of positive and negative interactions between functional sub-networks. This evidence stresses the importance of a whole-brain network modulation between coherent and non-coherent functional states. The disruption of the equilibrium between these two might lead to changes in levels of consciousness and, ultimately, to reduced levels of consciousness.

In fact, the *connICA* results presented in this paper depict a very challenging reality. Within the set of individual functional connectomes analyzed here, there is not just one but at least three independent mechanisms, namely FC-traits, whose predictability by consciousness related features is present but different on each one, and hence is most likely capturing different phenomena or mechanisms. A first *RSNs* trait only predicted by arousal, a very *sensitive* FC-trait, which isolates the functional connectivity blocks of typical RSNs present in an *alive and awake* brain (Figure 3D); a second *VIS-SM* trait, with predominant influence of visual and sensory regions, which links disruption of sensory networks to the CRS-R functional communication subscore (Figure 3E); a third *FP-DMN* trait, significantly associated to CRS-R sum of scores and communication, which stresses the key role of the negative connectivity between FP and DMN networks (Figure 3F) and inter-hemispheric communication (Figure 5 C,D) in the alteration of levels of consciousness.

The study presented here adds to recent studies from Iraji et al. (50), where ICA components of voxel-based functional connectivity were assessed, and from Misic et al. (51), where levels of integration of joint structural-functional connectivity patterns are assessed from sets of

individual connectomes by means of a single-value decomposition approach (47). Together with the methodology presented here, these recent efforts suggest that the area of Brain Connectomics is evolving into new data-driven ways of analyzing connectivity data at different spatial scales without stratifying subjects into *a priori* groups and hence, also without performing group-averages of individual connectivity matrices.

Our study has several limitations. The optimal size of the cohort for the extraction of the *connICA* components needs to be further investigated. Similarly, the best choice of the starting number of ICA components (here fixed to 15) and the threshold for the final selection of the most frequent components over multiple ICA runs (here fixed to 75%) need to be characterized in more detail. In this work we used the Shen parcellation (52) because of the uniformity of the size of brain regions and its functional data-driven approach. We also used the well-assessed RSNs decomposition provided by Yeo as obtained in a large cohort (n=1000) of healthy volunteers (31). However, other parcellations (53, 54) or finer decompositions (25, 26) might be beneficial in the *connICA* framework, depending on the research problem at hand and the desired level of spatial resolution.

Future work can be extended to the use of *connICA* for structural connectivity patterns, hence identifying SC-traits within a population of subjects. This approach is not limited to assessing consciousness, but has the potential of studying other progressive diseases and disorders, drug-induced effects (i.e. anesthesia), and also differences based on aging or gender. When associating traits with cognitive/clinical features, multi-linear models employed here can be expanded by allowing for non-linear terms and interactions, which could capture more complex associations between connectivity patterns and cognition.

In conclusion, we here proposed a novel data-driven approach, *connICA*, to extract the most influential connectivity patterns in the alteration of levels of consciousness. Our results shed light on isolating key functional core changes involved in the degradation of conscious states and establish links between isolated clinical/cognitive features and specific FC-traits.

Materials and methods

Subjects

The cohort studied here consists of 88 subjects with different levels of consciousness. From those, 32 were healthy controls (mean age 44 years ± 15 years, 21 males, 11 females). We selected 56 patients from an initial cohort of 216 patients in different levels of consciousness. Exclusion criteria were: i) neuroimaging examination in an acute state, i.e. <28 days from brain insult, ii) large focal brain damage, i.e. >2/3 of one hemisphere, as stated by a certified neuroradiologist, iii) suboptimal segmentation, normalization and/or parcellation of the brain volumes after visual inspection. Out of the selected 56, 39 were patients with disorders of consciousness (2 coma, 17 UWS, 20 MCS), 13 EMCS and 4 LIS. 28 out of 56 patients had traumatic brain injury (TBI), and 31 were sedated during the fMRI acquisition.

Healthy volunteers were free of psychiatric or neurological history. The study was approved by the Ethics Committee of the Medical School of the University of Liège. Written informed consent to participate in the study was obtained from the healthy subjects and from the legal surrogates of the patients.

Demographics

Nuisance variables included age, gender, etiology (1 for TBI, 0 otherwise), sedation (1 for sedated subjects, 0 otherwise) and the inverse of the time since the insult (in days), as we assumed healthy subjects' time since onset to be infinite and hence corresponds to zero in our codification.

To assess the level of consciousness, we used the scores obtained from the JFK Coma Recovery Scale-Revised (CRS-R) (32-34) assessment for each DOC patient. The CRS-R is the most sensitive and validated (55) scale to fully characterize and monitor DOC patients and provide a global quantification of their levels of consciousness. In particular, CRS-R integrates 25 arranged items that comprise 6 sub-scales addressing auditory, visual, motor, oromotor, communication, and arousal processes. Each item assesses the presence or absence of a specific physical sign that represents the integrity of brain function at one of four levels: generalized, localized, emergent, or cognitively mediated responsiveness. Scoring is based on the presence or absence of specific behavioral responses to sensory stimuli administered in a standardized manner. The reader can refer to (33, 34, 56) for a detailed description of the scale.

Image acquisition

Each subject underwent structural MRI and a 10 minute fMRI resting-state (task-free) session. Whole-brain structural MRI T1 data (T1-weighted 3D MP-RAGE, 120 transversal slices, repetition time = 2300 ms, voxel size = 1.0 x 1.0 x 1.2 mm^3, flip angle = 9°, field of view = 256 x 256 mm^2) and resting state BOLD fMRI data (Echo Planar Imaging sequence, gradient echo, volumes = 300, repetition time = 2000 ms, echo time = 30ms, flip angle = 78°, voxel size = 3 x 3 x 3 mm^3, field of view = 192×192 mm^2, 32 transversal slices) were acquired on a Siemens 3T scanner. Healthy subjects were instructed to keep eyes open during the fMRI acquisition.

Data processing and Functional Connectivity modeling

Data processing was performed by combining functions from FSL (57) and in-house developed Matlab (MATLAB 6.1, The MathWorks Inc., Natick, MA, 2000) code. The individual functional connectomes were modeled in the native BOLD fMRI space of each subject.

Processing steps were based on state of the art fMRI processing guidelines (58, 59). Structural images were first denoised to improve the signal-to-noise ratio (60), bias-field corrected, and then segmented (FSL FAST) to extract white matter, grey matter and cerebrospinal fluid (CSF) tissue masks. These masks were warped in each individual subject's functional space by means of subsequent linear and non-linear registrations (FSL flirt 6dof, FSL flirt 12dof and fnirt).

BOLD fMRI functional volumes were processed according to the steps recommended by (59). These steps included: slice timing correction, motion correction, normalization to mode 1000, demeaning and linear detrending, inclusion of 18 regressors consisting of 3 translations [x,y,z], 3 rotations [pitch, yaw, roll], and 3 tissue regressors (mean signal of whole-brain, WM and CSF), and the 9 corresponding derivatives (backwards difference, see Figure S1). A scrubbing procedure censoring high motion volumes was based on Frame Displacement (FD), DVARS and SD. FD measures the movement of the head from one volume to the next, and is calculated as the sum of the absolute values of the differentiated realignment estimates (by backwards differences) at every time-point (59); DVARS measures the change in signal intensity from one volume to the next, and is calculated as the root mean square value of the differentiated BOLD time-series (by backwards differences) within a spatial mask at every time-point (61); SD is the standard deviation of the BOLD signal within brain voxels at every

time-point (outlier volumes higher than 75 percentile +1.5 of the interquartile range were discarded, see Fig. S1).

A bandpass first-order Butterworth filter in forward and reverse directions [0.001 Hz, 0.08 Hz] was then applied. After that, the 3 principal components of the BOLD signal in the WM and CSF tissue were regressed out of the GM signal.

A whole-brain data-driven functional parcellation based on 278 regions, as obtained by Shen and colleagues (52), was first warped into each subject's T1 space (FSL flirt 6dof, FSL flirt 12dof and finally fnirt) and then into each subject's fMRI space. To improve the registration of the structural masks and the parcellation to the functional volumes FSL boundary-base-registration was also applied. Individual functional connectivity matrices (FC) were then estimated by means of pairwise Pearson correlations between the averaged signals of the regions of the parcellation, excluding the censored volumes as determined by the above-mentioned scrubbing procedure. Finally, the resulting FC matrices were ordered according to 7 resting-state sub-networks (RSNs) as proposed by Yeo and colleagues ((31), see insert of Fig 2B). For completeness, we added two more sub-networks: an 8^{th} sub-network representing the subcortical regions and a 9^{th} sub-network representing the cerebellum.

ConnICA: Independent component analyses of sets of individual functional connectomes

The input of ConnICA consists of all the individual FC profiles embedded into a dataset matrix where each row contains all the entries of the upper triangular part of the FC matrix for each subject (given the symmetry of FC) and hence provides an individual FC pattern. Note that this includes all FC matrices from all subjects, without any *a priori* information or any stratification of the data into groups (see scheme at Fig. 1). With this input, ICA decomposition of the FC patterns was applied by running fastICA algorithm (62) and setting the number of independent components to 15.

The output of connICA consists of two vectors per component. The first output vector will be referred to as *FC-trait*, which represents an independent pattern of functional connectivity. Interestingly, this vector can be represented back to its *spatial* form, i.e. a square symmetric matrix with brain regions in rows and columns. While the values here express connectivity units, they are not Pearson correlation coefficients and hence not restricted tothe [-1,1] range.

The second output vector is the weight of the FC-trait on each subject, which quantifies the prominence or presence of the trait in each individual FC matrix (note that this value can be positive or negative). In that sense, connICA is maximizing the individual variance explained by the multilinear regression of the obtained collection of FC-traits and subsequent subject weights.

Given the non-deterministic nature of ICA decomposition into components, we selected only the most robust ones (from now on simply denominated FC-traits), i.e. only those independent patterns that are frequently observed during the ICA decomposition of the FC data. To do so, instead of analyzing the connICA components from a single run, we evaluated the similarity of the *connICA* components over 100 runs. For an FC-trait to be robust, it has to appear (correlation of 0.75 or higher across runs) in at least 75% of the runs. This criterion resulted in 5 robust FC-traits. Each of these traits is obtained by averaging the correspondent "representations" found along the runs (see Fig. S2).

Each FC-trait was characterized by the mean and standard deviation of explained variance with respect to the individual FC matrices. The subject weights associated to each assessed FC-traits was then used as response in an incremental multi-linear regression model with up to 7 predictors. Predictors included the Coma Recovery Scale Revised (30) clinical subscores of each patient (Arousal, Auditory, Communication, Motor, Oromotor, Visual), and the sum of these scores. The control population was assumed to have the highest scores for each of the subscales. As aforementioned, the following variables were also included: age, gender, etiology (traumatic/non traumatic), sedation level and the inverse of the time since onset.

We then identified the FC-traits whose presence (weights) in individual FCs was significantly explained by a cognitive predictor (statistical significance set at p-value ≤ 0.05, Fig. 3G, 3H, 3I). The aim was to extract the connectivity patterns or traits associated to clinical features that go from wakefulness to the deepest level of unawareness.

Modularity analyses

Modularity is a measure of the strength of division of a network into modules or communities. Networks with high modularity have dense connections between the nodes within modules but sparse connections between nodes in different modules. The Newman-Girvan quality function Q is a way of quantifying network modularity. It is defined as the fraction of edges

that fall within modules minus the expected number of edges for a random graph with the same node degree distribution as the given network (29). Particularly, we here used the extension of Q for signed undirected networks proposed by Mucha et al. (30), and inspired by (63, 64).

To investigate the functional organization properties of the FC-traits extracted with connICA, we first assessed the similarity of each trait with Yeo's partitions using Newman-Girvan modularity function Q for signed undirected networks (30). In other words, we wanted to evaluate to what extent each FC-trait can be well-separated into communities based on a partition based on RSNs.

We then assessed the community structure of each FC-trait by using the Louvain method for identifying communities in large networks (36). In order to improve the stability of the community detection procedure, we performed consensus clustering (35) out of a set of 100 partitions obtained by the Louvain method. Consensus clustering is a technique that seeks for a median (or consensus) partition, i.e. the partition that is most similar, on average, to all the input partitions. The similarity can be measured in several ways, for instance co-occurrence of the nodes in the clusters of the input partitions (35). This "consensus" partition was finally selected as the most robust one.

Acknowledgements

We thank Marie-Aurelie Bruno, Athena Demertzi and Audrey Vanhaudenhuyse for help in acquiring the data. This research was supported by the This research was supported by the Belgian Funds for Scientific Research (FRS), European Commission, James McDonnell Foundation, European Space Agency, Belgian Science Policy (CEREBNET, BELSPO), Wallonia-Brussels Federation Concerted Research Action, Mind Science Foundation, Public Utility Foundation "Université Européenne du Travail" and "Fondazione Europea di Ricerca Biomedica", University and University Hospital of Liège. LH is a research fellow and SL a research director at FNRS.

References

1. Laureys S (2005) The neural correlate of (un)awareness: lessons from the vegetative state. *Trends Cogn Sci* 9(12):556-559.
2. Bernat JL (2009) Chronic consciousness disorders. *Annu Rev Med* 60:381-392.
3. Laureys S, Owen AM, & Schiff ND (2004) Brain function in coma, vegetative state, and related disorders. *Lancet Neurol* 3(9):537-546.
4. Giacino JT, Fins JJ, Laureys S, & Schiff ND (2014) Disorders of consciousness after acquired brain injury: the state of the science. *Nat Rev Neurol* 10(2):99-114.
5. Laureys S*, et al.* (2005) The locked-in syndrome: what is it like to be conscious but paralyzed and voiceless? *Progress in brain research* 150:495-611.
6. Giacino JT*, et al.* (1995) Recommendations for use of uniform nomenclature pertinent to patients with severe alterations in consciousness. *Archives of Physical Medicine and Rehabilitation* 76(2):205-209.
7. Boly M*, et al.* (2012) Brain connectivity in disorders of consciousness. *Brain Connect* 2(1):1-10.
8. Di Perri C, Stender J, Laureys S, & Gosseries O (2014) Functional neuroanatomy of disorders of consciousness. *Epilepsy Behav* 30:28-32.
9. Fernández-Espejo D*, et al.* (2012) A role for the default mode network in the bases of disorders of consciousness. *Annals of neurology* 72(3):335-343.
10. Owen AM, Schiff ND, & Laureys S (2009) A new era of coma and consciousness science. *Progress in brain research* 177:399-411.
11. Koch C, Massimini M, Boly M, & Tononi G (2016) Neural correlates of consciousness: progress and problems. *Nature Reviews Neuroscience* 17(5):307-321.
12. Bullmore E & Sporns O (2009) Complex brain networks: graph theoretical analysis of structural and functional systems. *Nat Rev Neurosci* 10(3):186-198.
13. Sporns O (2011) *Networks of the Brain* (MIT press).
14. Fornito A, Zalesky A, & Bullmore ET (2016) Fundamentals of Brain Network Analysis. (Academic Press).
15. van den Heuvel MP & Hulshoff Pol HE (2010) Exploring the brain network: a review on resting-state fMRI functional connectivity. *Eur Neuropsychopharmacol* 20(8):519-534.
16. Friston KJ, Frith CD, Liddle PF, & Frackowiak RS (1993) Functional connectivity: the principal-component analysis of large (PET) data sets. *J Cereb Blood Flow Metab* 13(1):5-14.
17. Fox MD*, et al.* (2005) The human brain is intrinsically organized into dynamic, anticorrelated functional networks. *Proc Natl Acad Sci U S A* 102(27):9673-9678.
18. Fox MD & Raichle ME (2007) Spontaneous fluctuations in brain activity observed with functional magnetic resonance imaging. *Nature Reviews Neuroscience* 8(9):700-711.
19. Calhoun VD, Liu J, & Adali T (2009) A review of group ICA for fMRI data and ICA for joint inference of imaging, genetic, and ERP data. *Neuroimage* 45(1 Suppl):S163-172.
20. Erhardt EB*, et al.* (2011) Comparison of multi-subject ICA methods for analysis of fMRI data. *Hum Brain Mapp* 32(12):2075-2095.
21. Greicius M (2008) Resting-state functional connectivity in neuropsychiatric disorders. *Curr Opin Neurol* 21(4):424-430.
22. Heine L*, et al.* (2012) Resting state networks and consciousness: alterations of multiple resting state network connectivity in physiological, pharmacological, and pathological consciousness States. *Front Psychol* 3:295.

23. Soddu A*, et al.* (2012) Identifying the default-mode component in spatial IC analyses of patients with disorders of consciousness. *Hum Brain Mapp* 33(4):778-796.
24. Vanhaudenhuyse A*, et al.* (2010) Default network connectivity reflects the level of consciousness in non-communicative brain-damaged patients. *Brain* 133(Pt 1):161-171.
25. Demertzi A*, et al.* (2014) Multiple fMRI system-level baseline connectivity is disrupted in patients with consciousness alterations. *Cortex* 52:35-46.
26. Demertzi A*, et al.* (2015) Intrinsic functional connectivity differentiates minimally conscious from unresponsive patients. *Brain* 138(Pt 9):2619-2631.
27. Achard S*, et al.* (2012) Hubs of brain functional networks are radically reorganized in comatose patients. *Proc Natl Acad Sci U S A* 109(50):20608-20613.
28. Crone JS*, et al.* (2014) Altered network properties of the fronto-parietal network and the thalamus in impaired consciousness. *Neuroimage Clin* 4:240-248.
29. Newman MEJ & Girvan M (2004) Finding and evaluating community structure in networks. *Physical review E* 69(2):026113.
30. Mucha PJ, Richardson T, Macon K, Porter MA, & Onnela J-P (2010) Community structure in time-dependent, multiscale, and multiplex networks. *science* 328(5980):876-878.
31. Yeo BT*, et al.* (2011) The organization of the human cerebral cortex estimated by intrinsic functional connectivity. *J Neurophysiol* 106(3):1125-1165.
32. Kalmar K & Giacino JT (2005) The JFK Coma Recovery Scale--Revised. *Neuropsychol Rehabil* 15(3-4):454-460.
33. Giacino J & Kalmar K (2006) Coma recovery scale-revised. *The Center for Outcome Measurement in Brain Injury*:36-51.
34. Schnakers C*, et al.* (2008) A french validation study of the Coma Recovery Scale-Revised (CRS-R). *Brain Injury* 22(10):786-792.
35. Lancichinetti A & Fortunato S (2012) Consensus clustering in complex networks. *Scientific reports* 2.
36. Blondel VD, Guillaume J-L, Lambiotte R, & Lefebvre E (2008) Fast unfolding of communities in large networks. *Journal of statistical mechanics: theory and experiment* 2008(10):P10008.
37. Honey CJ*, et al.* (2009) Predicting human resting-state functional connectivity from structural connectivity. *Proc Natl Acad Sci U S A* 106(6):2035-2040.
38. Vincent JL*, et al.* (2007) Intrinsic functional architecture in the anaesthetized monkey brain. *Nature* 447(7140):83-86.
39. Lutkenhoff ES*, et al.* (2015) Thalamic and extrathalamic mechanisms of consciousness after severe brain injury. *Annals of neurology* 78(1):68-76.
40. Crick F & Koch C (1995) Are we aware of neural activity in primary visual cortex? *Nature* 375(6527):121-123.
41. Dehaene S & Changeux JP (2011) Experimental and theoretical approaches to conscious processing. *Neuron* 70(2):200-227.
42. Boveroux P*, et al.* (2010) Breakdown of within- and between-network resting state functional magnetic resonance imaging connectivity during propofol-induced loss of consciousness. *Anesthesiology* 113(5):1038-1053.
43. Amico E*, et al.* (2014) Posterior cingulate cortex-related co-activation patterns: a resting state FMRI study in propofol-induced loss of consciousness. *PLoS One* 9(6):e100012.

44. Sämann PG*, et al.* (2011) Development of the brain's default mode network from wakefulness to slow wave sleep. *Cerebral cortex*:bhq295.
45. Boly M*, et al.* (2009) Functional connectivity in the default network during resting state is preserved in a vegetative but not in a brain dead patient. *Hum Brain Mapp* 30(8):2393-2400.
46. Di Perri C*, et al.* (2016) Neural correlates of consciousness in patients who have emerged from a minimally conscious state: a cross-sectional multimodal imaging study. *Lancet Neurol*.
47. Gazzaniga MS (2005) Forty-five years of split-brain research and still going strong. *Nature Reviews Neuroscience* 6(8):653-659.
48. Gazzaniga MS (2014) The split-brain: rooting consciousness in biology. *Proc Natl Acad Sci U S A* 111(51):18093-18094.
49. Marinsek N, Turner BO, Gazzaniga M, & Miller MB (2014) Divergent hemispheric reasoning strategies: reducing uncertainty versus resolving inconsistency. *Front Hum Neurosci*, Switzerland), Vol 8, p 839.
50. Iraji A*, et al.* (2016) The connectivity domain: Analyzing resting state fMRI data using feature-based data-driven and model-based methods. *Neuroimage*.
51. Misic B*, et al.* (2016) Network-Level Structure-Function Relationships in Human Neocortex. *Cereb Cortex*.
52. Shen X, Tokoglu F, Papademetris X, & Constable RT (2013) Groupwise whole-brain parcellation from resting-state fMRI data for network node identification. *Neuroimage* 82:403-415.
53. Desikan RS*, et al.* (2006) An automated labeling system for subdividing the human cerebral cortex on MRI scans into gyral based regions of interest. *Neuroimage* 31(3):968-980.
54. Gordon EM*, et al.* (2016) Generation and evaluation of a cortical area parcellation from resting-state correlations. *Cerebral cortex* 26(1):288-303.
55. Seel RT*, et al.* (2010) Assessment scales for disorders of consciousness: evidence-based recommendations for clinical practice and research. *Archives of physical medicine and rehabilitation* 91(12):1795-1813.
56. Giacino JT, Kezmarsky MA, DeLuca J, & Cicerone KD (1991) Monitoring rate of recovery to predict outcome in minimally responsive patients. *Archives of Physical Medicine and Rehabilitation* 72(11):897-901.
57. Jenkinson M, Beckmann CF, Behrens TEJ, Woolrich MW, & Smith SM (2012) Fsl. *Neuroimage* 62(2):782-790.
58. Power JD, Barnes KA, Snyder AZ, Schlaggar BL, & Petersen SE (2012) Spurious but systematic correlations in functional connectivity MRI networks arise from subject motion. *Neuroimage* 59(3):2142-2154.
59. Power JD*, et al.* (2014) Methods to detect, characterize, and remove motion artifact in resting state fMRI. *Neuroimage* 84:320-341.
60. Coupé P, Manjón JV, Robles M, & Collins DL (2012) Adaptive multiresolution non-local means filter for three-dimensional magnetic resonance image denoising. *Image Processing, IET* 6(5):558-568.
61. Smyser CD, Snyder AZ, & Neil JJ (2011) Functional connectivity MRI in infants: exploration of the functional organization of the developing brain. *Neuroimage* 56(3):1437-1452.
62. Hyvarinen A (1999) Fast and robust fixed-point algorithms for independent component analysis. *IEEE Trans Neural Netw* 10(3):626-634.

63. Gómez S, Jensen P, & Arenas A (2009) Analysis of community structure in networks of correlated data. *Physical Review E* 80(1):016114.
64. Traag VA & Bruggeman J (2009) Community detection in networks with positive and negative links. *Physical Review E* 80(3):036115.

Figure Legends

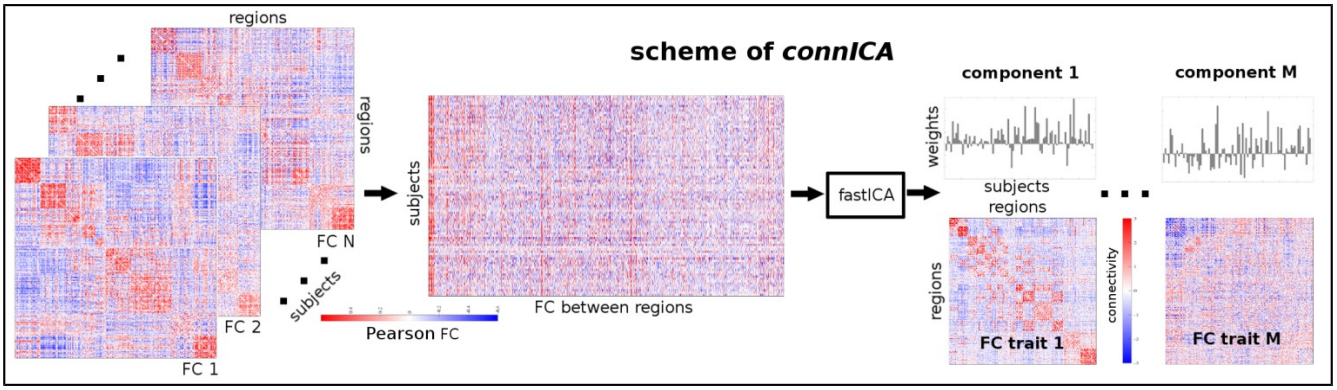

Figure 1. Workflow scheme of the proposed Connectivity Independent Component Analysis (*ConnICA*). The *N* individual functional connectivity (FC) matrices (left) are concatenated into a matrix where rows are the subjects and columns are the functional connectivity entries in the FC matrix). The ICA algorithm extracts the M independent components (i.e. functional traits) associated to the whole population and their relative weights across subjects. Colorbars indicate positive (red) and negative (blue) connectivity values, being Pearson's correlation coefficient values in the case of individual FC matrices (left side of scheme), and unitless connectivity weights in the case of FC-traits (right side of the scheme).

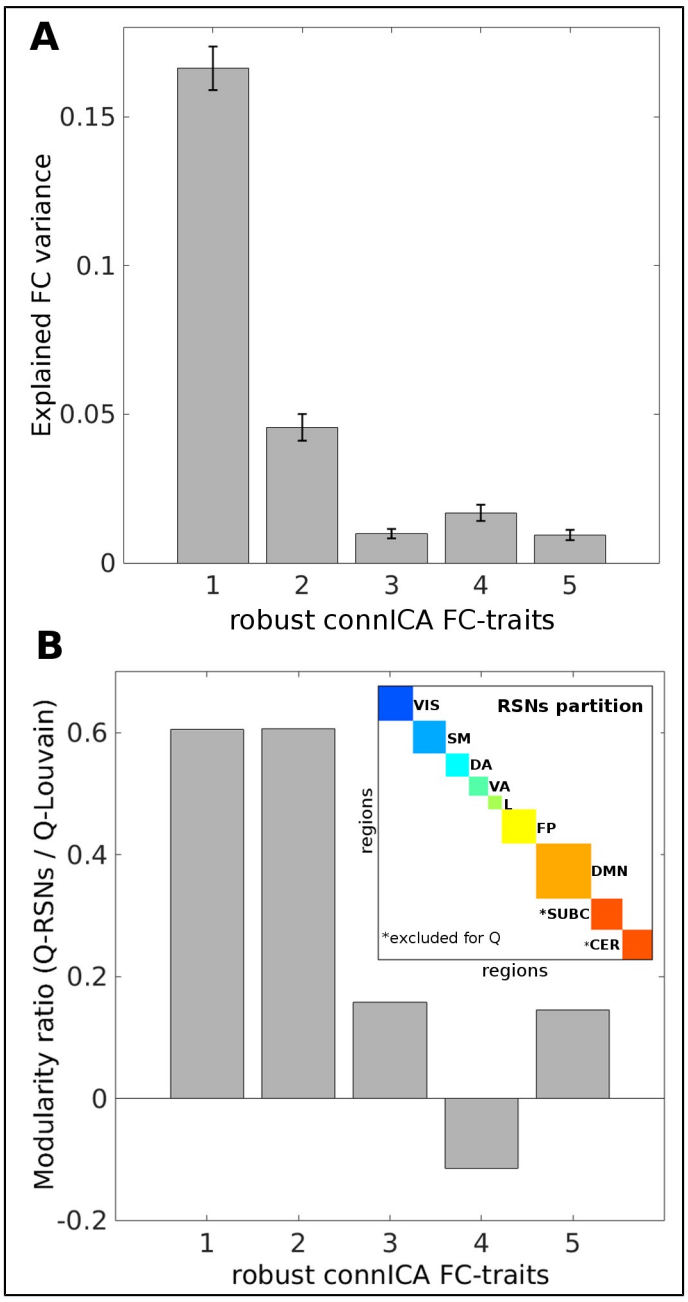

Figure 2. *connICA*-extracted robust FC traits A) Bar plot of the explained FC variance for the 5 most robust traits extracted with *connICA*. Error bars show the standard error across subjects. **B)** Bar plot of the modularity ratio for the 5 robust FC-traits extracted with connICA. This ratio is defined as the quality function Q ((30), see Materials and Methods) for the imposed a priori Resting State Networks' (RSNs) partition (encompassing 7 networks: visual (VIS), sensorimotor (SM), dorsal attention (DA), ventral attention (VA), limbic (L), fronto-parietal (FP), default mode network (DMN), see top right insert in panel B), divided by the quality function Q (30) for the data-driven partition obtained from consensus clustering (35) and Louvain~~'~~ algorithm (36).

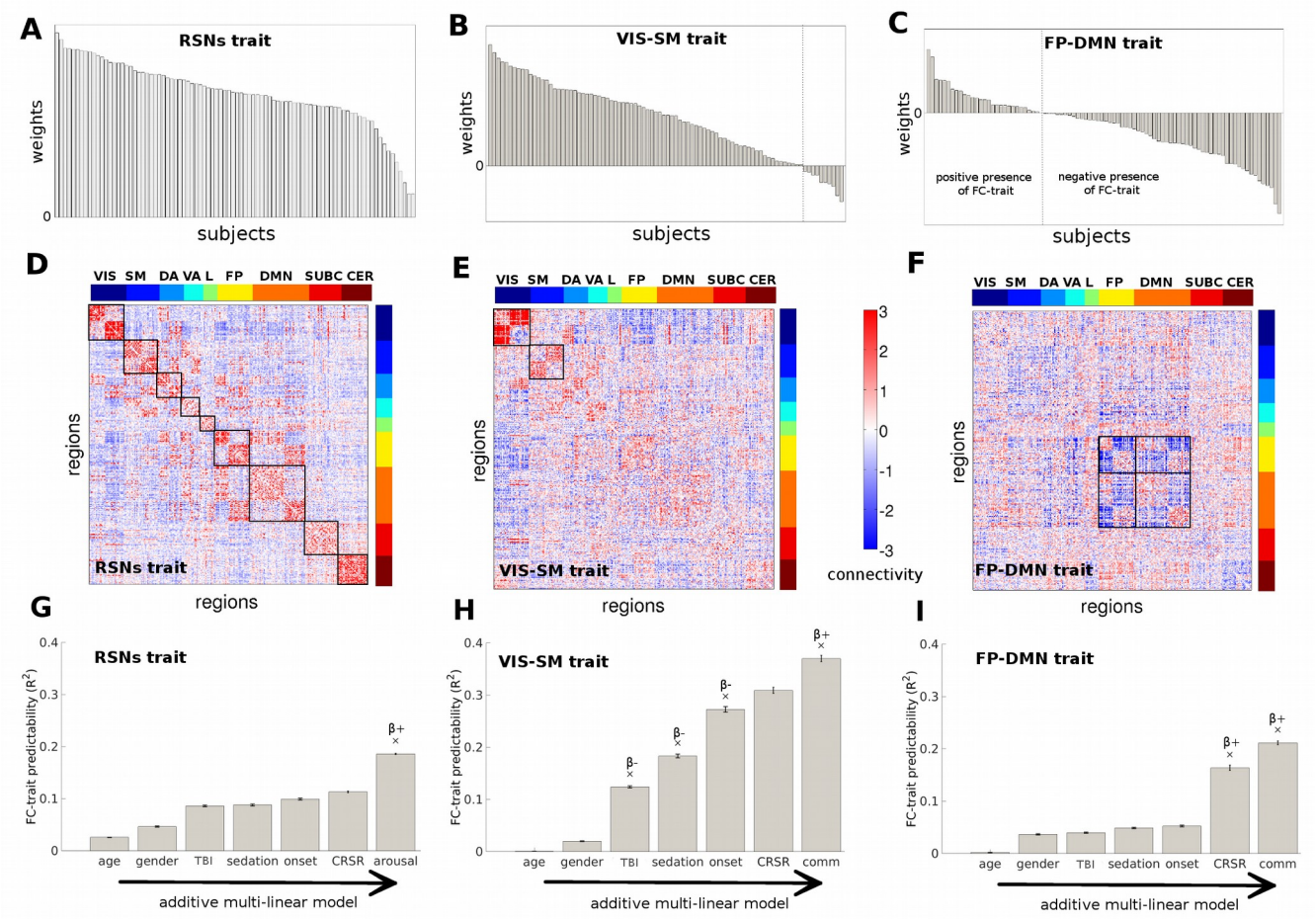

Figure 3 Mapping of the three main functional traits and their predictability by consciousness features. **A-C)** Quantified presence of each FC-trait on each individual functional connectome. Subject weights are sorted from greater to smaller on each FC-trait. **D-F)** Visualization of the three FC-traits associated to consciousness features. The brain regions are ordered according to Yeo's (31) functional RSNs as indicated : Visual (V), Somato-Motor (SM), Dorsal Attention (DA), Ventral Attention (VA), Limbic system (L), Fronto-Parietal (FP), Default Mode Network (DMN), and for completeness, also subcortical regions (SUBC) and cerebellum (CER). **G-I)** Bar-plot of the FC-traits predictability based on additive multi-linear regression models when predictors are sequentially introduced in the following order: age, gender, trauma, sedation, inverse of the time since onset, Coma Recovery Scale – Revised (CRS-R) total scores and the CRS-R communication subscore. Error bars show the standard error across the 100 ICA runs. Crosses on the top of a bar indicate that the inclusion of the correspondent predictor significantly increased the predictability of the model. The sign of the beta coefficient associated to each significant variable is shown below each asterisk, indicating whether there is a negative or positive trend with respect to the weights of the FC traits.

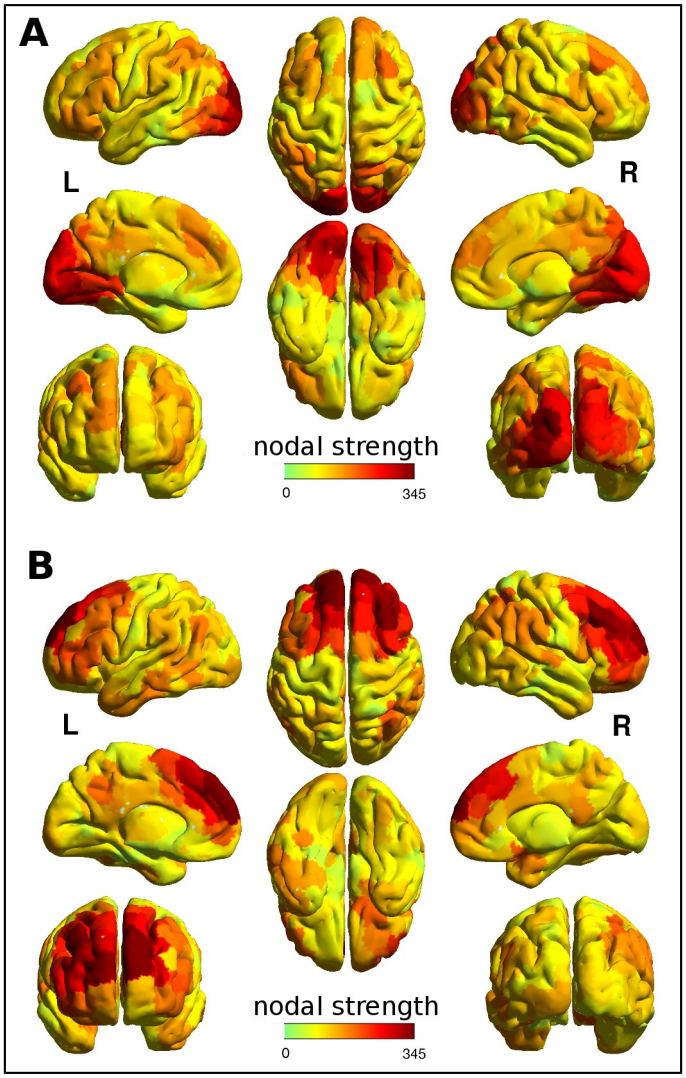

Figure 4. The strength per region computed as absolute sum of component weights allows an assessment of the overall centrality of each region for **A)** VIS-SM trait and **B)** FP-DMN trait.

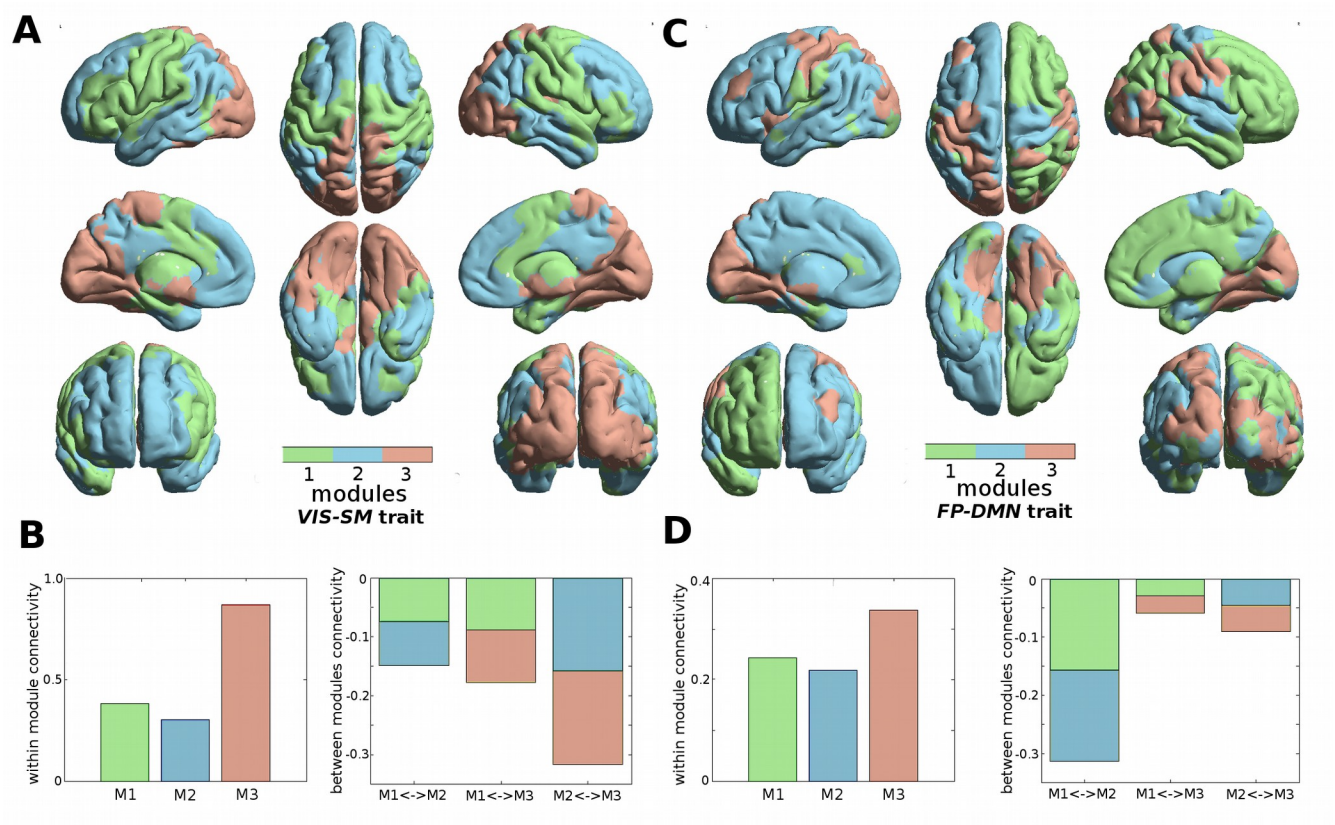

Fig. 5 A) Brain render of the modules obtained on *VIS-SM* trait (see Materials and Methods). Each color represents region's membership in a module. **B)** Left: bar plot of the average weight within each module in *VIS-SM* trait. Right: bar plot of the average between-module weight in *VIS-SM* trait. **C)** Brain render of the modules obtained on *FP-DMN* trait. **D)** Left: bar plot of the average weight within each module in *FP-DMN* trait. Right: bar plot of the average between-module weight in *FP-DMN* trait.

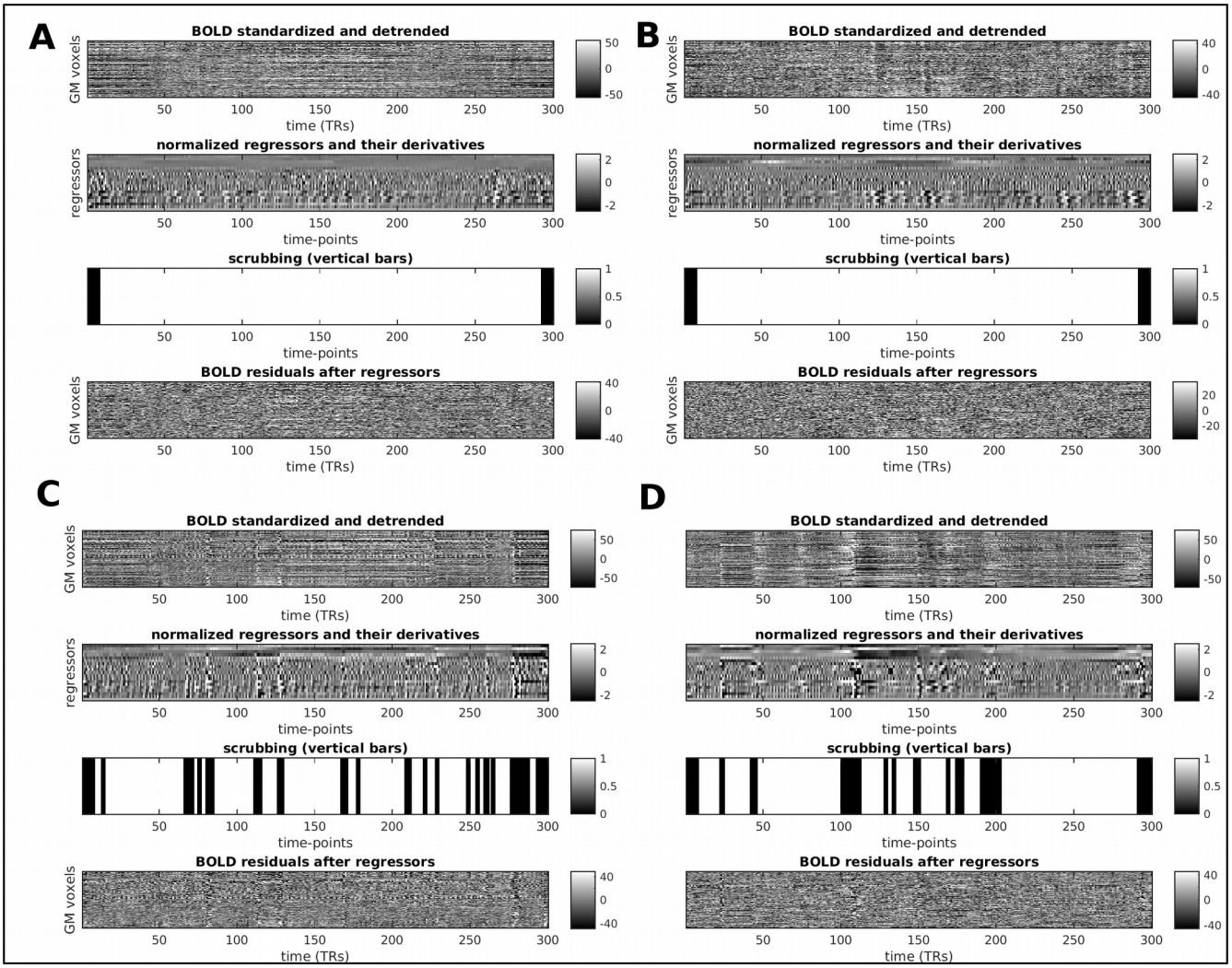

Figure. S1: Illustration of the fMRI preprocessing steps described in the Materials and Methods section on four subjects. Task-free session for four single subjects (A-D). For each subject, the 4 plots from top to bottom: 1) The fMRI time courses in GM voxels after slice timing and motion correction, normalization to mode 1000, demeaning and detrending; 2) The 18 motion and physiological noise regressors; [x, y , z, pitch, yaw, roll], the tissue mean signal of whole-brain, WM and CSF and their corresponding nine derivatives (backwards difference); 3) Visual representation of the scrubbing procedure based on Frame Displacement (FD), DVARS and SD to drop or censor volumes with motion (indicated by the dark vertical bars) from the computation of the pairwise correlations; 4) Residuals of the BOLD time courses of GM voxels after regressing out the 18 regressors. Subjects A and B had no censored volumes, with C and D having 14% and 11% censored volumes, respectively. Note that first and last 7 volumes in each session were always excluded.

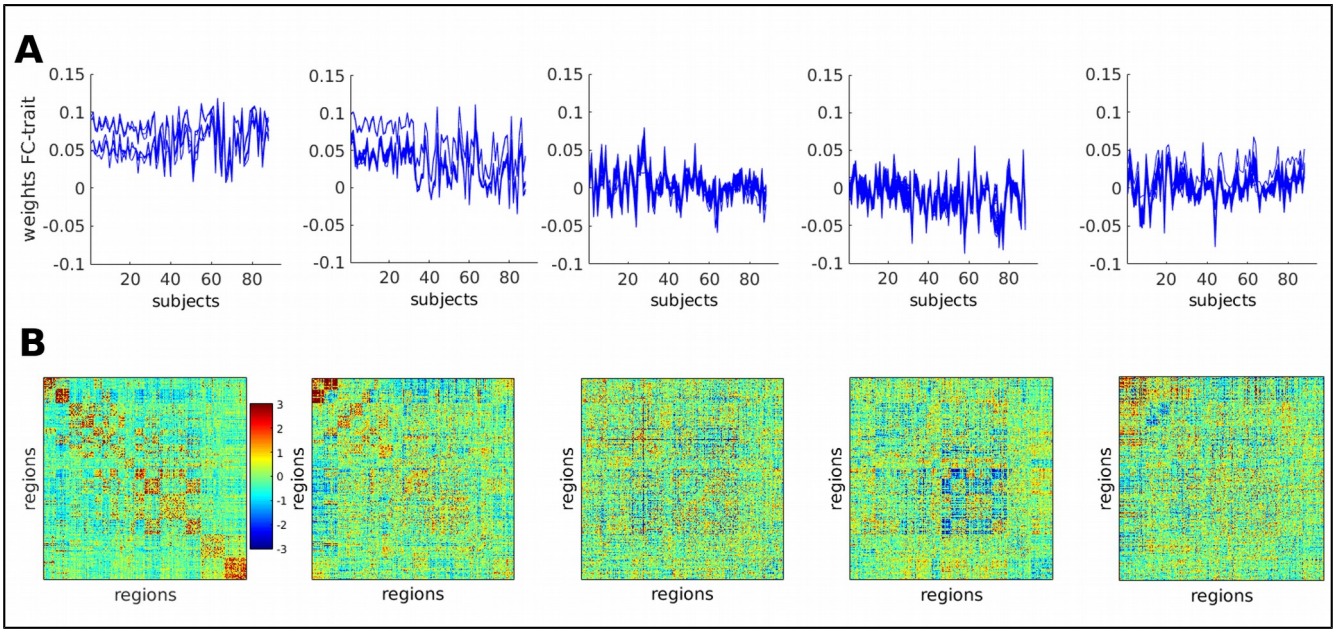

Figure S2: **A)** Plot of the correspondent weights per subjects for each single connICA run. **B)** Plot of the five robust connectivity traits extracted using connICA based on 100 runs. Only three of the FC traits were associated with cognitive scores linked to levels of consciousness.